Talanta 104 (2013) 58–66

Contents lists available at SciVerse ScienceDirect

Talanta

journal homepage: www.elsevier.com/locate/talanta

CIE$L^*a^*b^*$ color space predictive models for colorimetry devices – Analysis of perfume quality

Rabia Korifi [a,b,*], Yveline Le Dréau [a], Jean-François Antinelli [b], Robert Valls [a], Nathalie Dupuy [a]

[a] Laboratoire LISA, EA 4672 Equipe METICA, Case 451, Aix-Marseille Université, 13397 Marseille Cedex 20, France
[b] Analytics Consulting, 22 Parc Lubonis 06000 Nice, France

ARTICLE INFO

Article history:
Received 21 May 2012
Received in revised form
8 November 2012
Accepted 11 November 2012
Available online 23 November 2012

Keywords:
Colorimetry
Spectrophotometry
CIELAB
Predictive models
Quality control
Fragrances

ABSTRACT

Color perception plays a major role in the consumer evaluation of perfume quality. Consumers need first to be entirely satisfied with the sensory properties of products, before other quality dimensions become relevant. The evaluation of complex mixtures color presents a challenge even for modern analytical techniques. A variety of instruments are available for color measurement. They can be classified as tristimulus colorimeters and spectrophotometers. Obsolescence of the electronics of old tristimulus colorimeter arises from the difficulty in finding repair parts and leads to its replacement by more modern instruments. High quality levels in color measurement, i.e., accuracy and reliability in color control are the major advantages of the new generation of color instrumentation, the integrating sphere spectrophotometer. Two models of spectrophotometer were tested in transmittance mode, employing the d/0° geometry. The CIE$L^*a^*b^*$ color space parameters were measured with each instrument for 380 samples of raw materials and bases used in the perfume compositions. The results were graphically compared between the colorimeter device and the spectrophotometer devices. All color space parameters obtained with the colorimeter were used as dependent variables to generate regression equations with values obtained from the spectrophotometers. The data was statistically analyzed to create predictive model between the reference and the target instruments through two methods. The first method uses linear regression analysis and the second method consists of partial least square regression (PLS) on each component.

1. Introduction

Color of foods, fragrances and cosmetics is the first contact point of the consumer with it, so it strongly influences consumers' preferences. Color has a major role in the acceptability of the product and is related to the consumer perception of flavor, sweetness, scents and other physical properties in relation to the quality of the product [1–4]. Manufacturers have been aware of this for a long time, which explains their efforts to assess and control the color of their products. Since the perception of color mainly depends of the observer and other illumination conditions, an objective assessment of color requires appropriate instrumentation that follows the recommendations instituted by the CIE (International Commission on Illumination). Consumer choice depends on the quality of the product, the color has such a psychological impact on the consumer that it is directly associated to the quality of the product. Thus, the implementation of instrumental measurements of color for the quality control is correlated to the consumer choice [5–9].

In the case of the creation of perfumes, one of the most current physicochemical analysis assured by the control laboratory is the color measurement of raw materials, bases and products. The engineering properties [10] of perfumes are important, if not essential, in the process design and manufacture of perfume products. Color, gloss and translucency are the optical properties that could be viewed by the consumer as an aspect of the global quality. Perfumers have to match the product quality with specific requirements of the consumer and the feedback obtained by market research tools.

From the early 1980s to the end of the 1990s, the colorimeter used for perfumers consists in a device with three sensors filtered, which give the relative amounts of the three primary colors required for a color match, red, green and blue. However, because of its discontinuation of technical support and repair parts, this device became obsolete. From now on, the colorimeter consists in a modern equipment more available on the market, an integrating sphere spectrophotometer with multichannel detector. The

* Corresponding author at: Laboratoire LISA, Equipe METICA EA 4672, Case 451, Aix-Marseille Université, Campus de St Jérôme, Avenue Escadrille Normandie Niemen, 13397 Marseille Cedex 20, France.
E-mail addresses: rabia.korifi@yahoo.fr (R. Korifi), yveline.le-dreau@univ-amu.fr (Y. Le Dréau), jfantinelli@analytics-consulting.fr (J.-F. Antinelli), nathalie.dupuy@univ-amu.fr (N. Dupuy).

0039-9140/$ - see front matter © 2012 Elsevier B.V. All rights reserved.
http://dx.doi.org/10.1016/j.talanta.2012.11.026

benefit of this new generation of device lies in its long-term stability, in contrast to filter device, no alteration phenomenon is observed. This instrumentation with improved sensor technology allows a more accurate and reproducible determination of the color space parameters [11].

To objectively define a color, in addition to using appropriate instrumentation, it is necessary to follow the recommendations established by the CIE. The CIE recommends a particular illuminant/observer combination and color spaces (CIEXYZ, CIE$L^*a^*b^*$) purposed at standardize the definition of color and provide more uniform color differences in relation to visual differences.

The quality control is the way to control process variation for assuring the production quality against design tolerances. It is based on the large amount of data collected over time with the reference instrument, the tristimulus colorimeter device. From these database, tolerances have been defined on each type of products for the three CIE color space parameters L^*, a^* and b^*. Control maps have been created from the tolerances, though these control maps are device-specifics. Thus, when using a new device, the measured $L^*a^*b^*$ parameters are not exactly the same, so it is excluded to use the same control maps for the quality control. Then, it becomes necessary to go to establish correlations between measurements made on different devices in order to continue using the same card control. In theory, there should not be any differences between the results obtained by colorimetry and by spectrophotometry. However, in practice, despite the fact that working properly with both types of instruments well calibrated, differences in responses affect the process of quality control. These differences affect even more the samples subjected to small tolerance ranges than those subject to greater tolerance ranges. Indeed, in the case of small ranges of tolerances, differences will result in an easier passage in non-conformity of the sample, previously tested in accordance with the reference method. From a purely practical point of view, the industrial is interested to have, from his new device, the same back line that with his former device. The goal is to maintain its database acquired over 25 years.

There are few scientific publications on correlations between measurements. Buslig [12] worked on the comparison of a tristimulus colorimeter and a sphere spectrophotometer for the measurement of orange juice color by tristimulus *XYZ* values correlation. Fullerton and Keiding [13] made a comparison between a tristimulus colorimeter and two spectrophotometers for the analysis of skin color by $L^*a^*b^*$ parameters correlation. In the two studies, the measurements were made by reflectance mode, which is in accordance to the CIE standards for opaque samples. The results are that satisfactory correlation coefficients were established by regression analysis. Nevertheless, these studies only refer to reflectance mode for opaque samples while many products requiring color measurement such as raw materials for perfumes are transparent and reflectance mode is not suitable for this determination. Furthermore, a review on instrumental measurement of orange juice color [14] states that it was demonstrated that color measurement by transmission was not effective due to its lack of reproducibility.

In this study, two bench-top spectrophotometers have been tested; these instruments are designated as targets instruments. The choice of the spectrophotometers has been done according to a set of specifications gathering the necessary technical features for a spectrophotometer. Suppliers were contacted to choose the spectrophotometer that best meets these criteria. These selection criteria were, among others, the types of illuminants, the measurement time, the size of sample cell supported, the color spaces available for the calculation, and finally a very important point, the access to spectral curves and to integrals values. Several spectrophotometers of different brands have been selected and the final choice was done according to their availability for rental.

For direct comparison between the colorimeter and the spectrophotometers devices, results were measured in CIE$L^*a^*b^*$ color space. The aim of this study is to be able to predict from the measured values of the target instruments, the $L^*a^*b^*$ values that would have been obtained on the reference instrument in order to keep the current control maps. For this, the procedure is to establish the best prediction model between the reference instrument and the target ones.

2. Theory

2.1. Basic color concepts

2.1.1. What is color?

The notion of color is based on three criteria: the hue (shade), the lightness (brightness) and the saturation (intensity). These three elements are the three color attributes, and can be put together to create the three-dimensional color solid shown in Fig. 1(a) [15].

In the construction of the three-dimensional solid, hues are the outer rim of the solid, lightness increases or decreases along the vertical axis and saturation varies according to the central point. Value scales were created to define these criteria, many methods have been developed to quantify color and to allow to express it with greater ease and precision.

2.1.2. Space for measuring color

Several systems for expressing color numerically were developed by an international organization concerned with issues of lighting and color, the International Commission on Illumination (CIE). One of the best known of these systems is the $L^*a^*b^*$ color space (also referred to as CIELAB) devised in 1976 [16]. In this space as seen in Fig. 1(b), L^* indicates lightness, its value extended from 0 (black) to 100 (white). a^* and b^* are the chromaticity coordinates. The a^* and b^* indicate color directions: $+a^*$ is the red direction, $-a^*$ is the green direction, $+b^*$ is the yellow direction, and $-b^*$ is the blue direction. The center is achromatic, as the a^* and b^* values increase and the point moves out from the center, the saturation of the color increases.

The color is represented by a point in this space, which allows high precision in the definition of this one. The values of L^*, a^*, and b^* are proportional to the tristimulus values *XYZ* [17] and to X_n, Y_n and Z_n, which are the tristimulus values *XYZ* of a perfect reflecting diffuser, set by the CIE in 1931, as seen in the transfer Eqs. (1–3).

$$L^* = 116 \times \left(\frac{Y}{Y_n}\right)^{1/3} - 16 \tag{1}$$

$$a^* = 500\left[\left(\frac{X}{X_n}\right)^{1/3} - \left(\frac{Y}{Y_n}\right)^{1/3}\right] \tag{2}$$

$$b^* = 200\left[\left(\frac{Y}{Y_n}\right)^{1/3} - \left(\frac{Z}{Z_n}\right)^{1/3}\right] \tag{3}$$

2.2. Principle of colorimetry

The principle of colorimetry is based on the tristimulus method [18], i.e., each color is the combination in different proportions of red, green and blue. For one color, the colorimeter gives the percentages of the three primary colors. A set of three sensors filtered to have nearly the same color sensitivity as the human eye, receive light from the object and transmit the

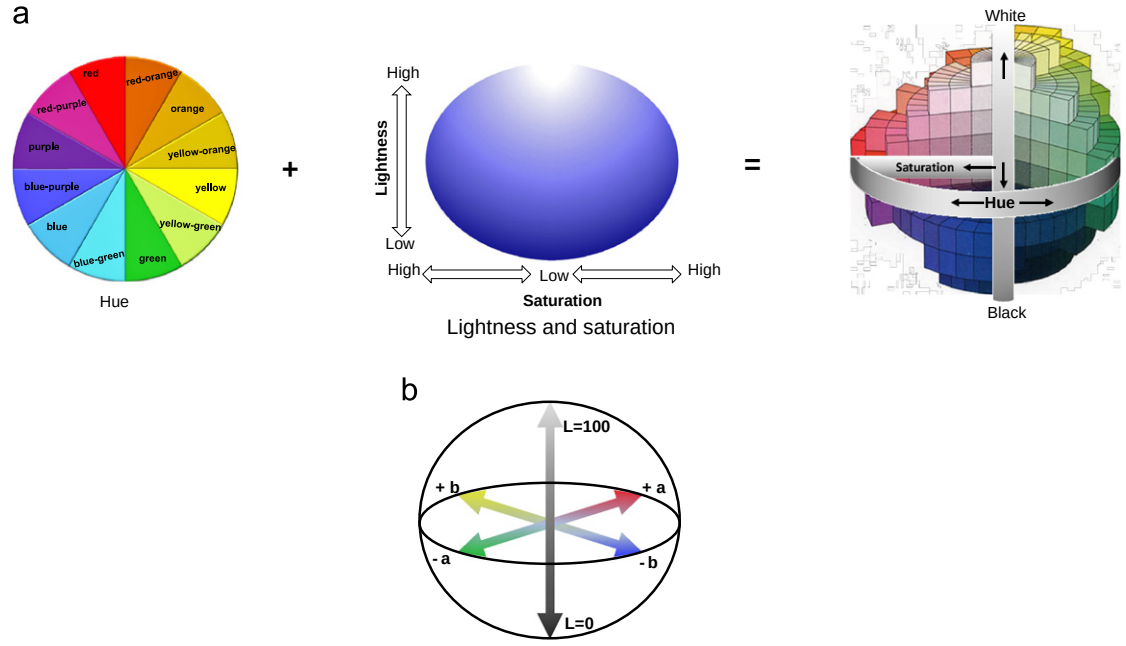

Fig. 1. (a) Creation of three-dimensional color solid; (b) CIELAB color space. (For interpretation of the references to color in this figure legend, the reader is referred to the web version of this article).

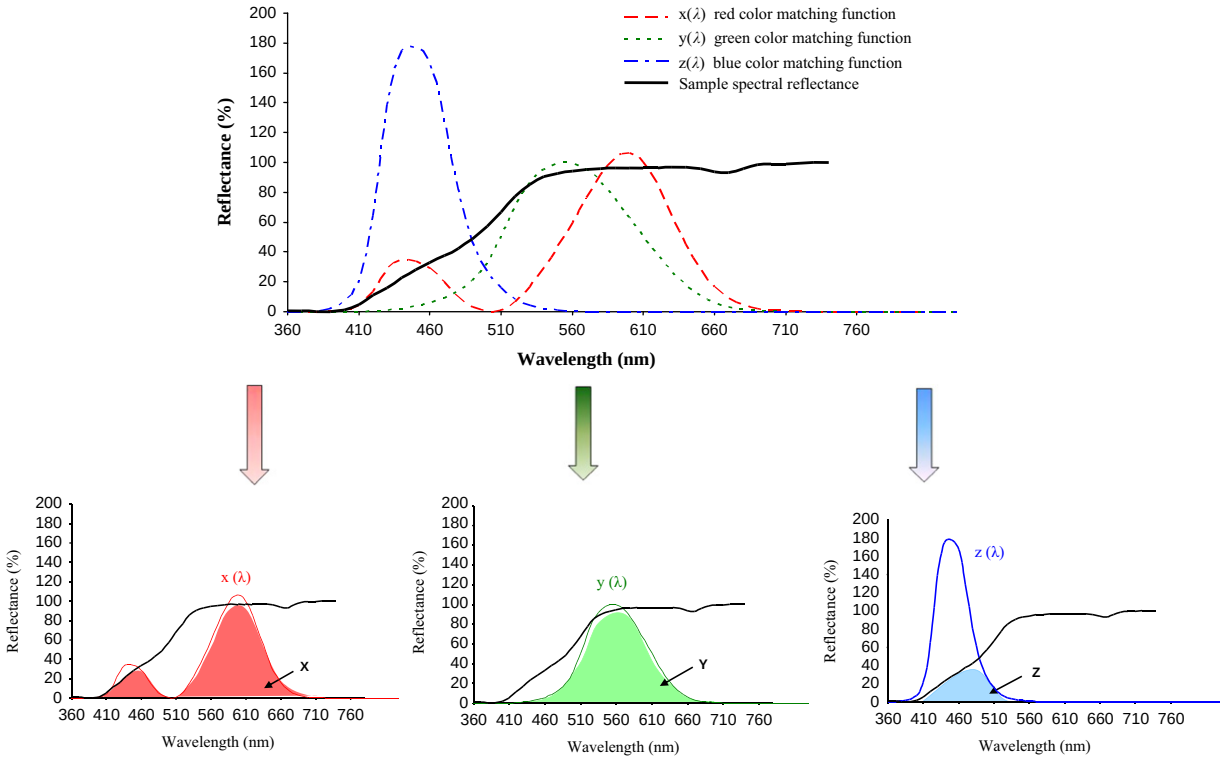

Fig. 2. Determination of tristimulus values in spectrophotometry from the superposition of the spectral reflectance of the sample and the color matching functions $x(\lambda)$, $y(\lambda)$, $z(\lambda)$ corresponding to the human eye perception. (For interpretation of the references to color in this figure legend, the reader is referred to the web version of this article).

information to the data processor that determines the tristimulus values *XYZ* by the standards of the CIE.

2.3. *Principle of spectrophotometry*

Multiple spectral sensors receive light from the object and transmit the information to the microprocessor. For each wavelength in the visible light range, the spectral reflectance is measured [19]. From the spectral data, the tristimulus values *XYZ* are calculated by integration. *XYZ* tristimulus values are equal to the integration of the shaded areas in the spectral reflectance curve of the object (Fig. 2). In addition to display numerical color data, a spectrophotometer can also display a graph of the spectral reflectance to provide more detailed information about the nature of the color.

3. Materials and method

3.1. Samples

Three hundred and eighty samples were measured with each instrument. The samples are raw materials and bases used in the preparation of perfumes, as well as finished products. Samples are filled into a 10 mm thick and 5 cm long cell made of ordinary glass. To each category of samples corresponds a tolerance range for the parameters values $L^*a^*b^*$. If at least one value is out of range, the sample is considered as non conform.

3.2. Tristimulus colorimeter vs spectrophotometers

The experimental reference device, the Konica Minolta CT310 is a transmission tristimulus colorimeter used to measure transparent colors of fluids. The lighting is provided by a pulsed xenon arc lamp using illuminant D65 [20], the detector consists of three sensors corresponding to the cones of the human eye that measure the light reflected from the sample with diffuse illumination/0° viewing angle geometry [21]. Then the tristimulus values are calculated by the built-in data processor. Two spectrophotometers are tested, the Konica Minolta CM-3600d and the HunterLab UltraScan Vis. The spectrophotometers incorporate sphere optics and four pulsed xenon lamps, covering the entire visible spectrum.

The instruments are used in transmission mode, the light from the lamps passes through a diffuser, illuminating the interior surface of the integrating sphere. The sample is indirectly illuminated by light reflected from the sphere walls with diffuse illumination/0° geometry. Light reflected from the sample is directed through lens system to a diffraction grating. The grating disperses the spectrum and reflects it through an integrating lens to a dual 40-elements silicone photodiode arrays detector. The spectral reflectance of the sample is measured between 360 and 740 nm with a resolution of 10 nm. The signals from the detector array are processed by a data processor to yield the appropriate color scale values. The instruments are controlled by the computer with the SpectraMagic NX proprietary software for the CM-3600d and with the EasyMatch QC proprietary software for the UltraScan Vis.

Systems were calibrated with a white calibration plate, using illuminant D65 before each sample analysis. The area of measurement is 20 mm for the colorimeter, 17 mm for the Konica spectrophotometer and 19 mm for the HunterLab spectrophotometer. The distance between the sample and the exit window of light is 1 cm for CT310 colorimeter, and 1.5 cm for the both spectrophotometers. Results were measured in CIE$L^*a^*b^*$ units for direct comparison with the analogous colorimeter values. Each sample was measured three times to assess the repeatability of the measurement and the possible variations of integrals. The repeatability being almost perfect, an average of these measurements was done. The measurement time is 2 s for the three instruments and the time interval between two measurements is 3 s.

Apart from this, it is of vital importance to define the correct conditions of the measurements, not only the standard observer and illuminant established by the CIE, but also the arrangement of the sample, related to the geometry of the system, the light source intensity, and the blank measurement, among others. Differences of responses between the two types of instrument can be due to differences in taking the white reference spectrum. However, it is impossible because of the technical constraints of the device to interchange the white calibration plates serving as reference white that are unique for each instrument.

3.3. Data processing

Two methods of data processing are tested. The first method uses simple linear regression analysis to explore and model the functional relation between the colorimeter $L^*a^*b^*$ space color and the spectrophotometer one. Then the regression model is used to make predictions.

The second method consist of create predictive models by partial least square regression (PLS) on each parameter [22]. Most commonly used in spectrometric analyzes, PLS can be used to predict a set of dependent variables from a large set of explanatory variables (predictors) that can be highly correlated. PLS is the most popular method in the literature because it usually provides better results that other multiple regression methods. This supervised analysis is based on the relation between the reflectance spectra and the $L^*a^*b^*$ parameters of the sample. Overlapping of the spectral information may be overcome by using this powerful multicomponent analysis. The method allows a sophisticated statistical approach using the full spectral region rather than one space color value. The algorithm is based on the ability to mathematically correlate spectral data to a property matrix of interest while simultaneously accounting for all other significant spectral factors that perturb the spectrum. It is a multivariate regression method that uses the full spectral region and is based on the use of latent variables. Its construction is divided into two stages. The calibration step allows to construct the calibration equation, i.e., the mathematical model that correlates the input variables X (reflectance spectra) and the responses Y predicting (values of $L^*a^*b^*$). The number of latent variables selected for the PLS model was obtained by full cross validation on the calibration set, allowing an unbiased estimate of the validation error. The prediction step is the use of the model to predict the response (Y) of another batch of samples. The 2 batches of samples were as follows: 255 samples for calibration, selected randomly into the full ranges of values, and 125 samples for the prediction (25 samples each of 5 batches of samples received), also selected to cover the entire range of values.

The evaluation of the errors in the calibration is estimated by computing the standard error of calibration (SEC) for each parameter $L^*a^*b^*$. The calculation of the SEC is given by the Eq. (4).

$$\mathrm{SEC} = \sqrt{\left(\frac{\sum_{i=1}^{N}(y_i - y_i')^2}{N-1-p}\right)} \tag{4}$$

where y_i is the known value, y'_i is the calculated value, N the number of samples and p is the number of independent variables.

The standard error of prediction (SEP) gives an estimation of the prediction performance during the step of validation (Eq. (5)).

$$\mathrm{SEP} = \sqrt{\left(\frac{\sum_{i=1}^{M}(y_i - y_i')^2}{M}\right)} \tag{5}$$

where M is the number of samples in the prediction set.

Another useful parameter is the relative error of prediction (REP) that shows the predictive ability of the model, shown in Eq. (6).

$$\mathrm{REP} = \frac{\mathrm{SEP}}{\bar{y}} \times 100 \tag{6}$$

where $\bar{y}$ is the mean of the known values.

As the SEP is a standard deviation, the $(\mathrm{SEP})^2$ can be considered as a variance and, in a first approximation, can be analyzed as such. The Fisher–Snedecor test allows a comparison between the predictive qualities of two models with $(\mathrm{SEP})^2_0$ the smallest

$(SEP)^2$ such as the Eq. (7):

$$F = \frac{(SEP)^2}{(SEP)^2_0} < F_c \quad (7)$$

where F_c is the critical value provided by the Fisher–Snedecor tables for the number of degrees of freedom of the SEP. This test will be applied to compare the prediction performance of the two spectrophotometers.

The predictive ability of the model should also be expressed by the square of correlation coefficient (R^2) also called determination coefficient. The regression coefficients are the numerical coefficients which express the link between the predictor variations and the response variations.

The chemometric applications were performed by The Unscrambler® version 9.2 developed by CAMO (Computer Aided Modelling, Trondheim, Norway).

4. Results and discussion

The first analytical step is to examine the data by comparing the reference instrument data with those of the target instruments and to determine the level of agreement between the data obtained by the two instruments. Three levels of agreement exist: equivalence, commutability and incompatibility. If the results are identical to the analytical imprecision close, both instruments are equivalent and can be exchanged without loss of accuracy. If the results are identical at the close tolerance, they are not strictly equivalent, instruments are said commutable. Finally, if they produce results that differ more than the allowed tolerance for the parameter, the instruments are incompatible. According to Bland and Altman [23], the best statistical approach is not obvious. The usual method is to calculate the correlation coefficient between the two instruments data, but the use of correlation coefficient as an indicator of agreement is not sufficient. In this study, their alternative approach based on graphical techniques is tested as a measuring agreement. First, the data is plotted and a line of equality is drawn (Fig. 3). This line represents the ideal case where the two instruments gave exactly the same results for each sample. It helps to visually evaluate the degree of agreement between the two instruments. Then, the regression lines are drawn and the correlation coefficients r are calculated between the two instruments. For the data in Fig. 3, $r_{L^*}=0.96$, $r_{a^*}=0.67$ and $r_{b^*}=0.97$. The hypothesis is that the measurements by the two instruments are linearly related for L^* and b^* but nor for a^*. This could be explained by the fact that L^* is linearly related to Y (Eq. (1)) and that the participation of Z in the calculation of b^* is very low compared to Y (Fig. 3) so that the Eq. (3) is nearly a linear relation of Y. However, a^* depends as much on X than on Y. The low correlation coefficient of a^* already shows a lack of agreement. Though, even if the parameters L^* and b^* show high correlations, this does not necessarily mean that the two instruments are in agreement. Indeed, r is defined by measuring the strength of a relation between two variables, not the agreement between them. There is a perfect agreement only if the points in Fig. 3 lie along the line of equality, but there is a perfect correlation if the points lie along any straight line; that is to say if the regression line is equal to the line of equality.

A useful start is to draw a simple plot of the results of one instrument against those of the other (as done on Fig. 3) but usually the data points will be clustered near the regression line and it will be difficult to assess between-spectrophotometer differences. A plot of the difference between the data of the spectrophotometers against their mean may be more informative. The difference in value between target and reference is deferred in ordinate and the average of these two values on the abscissa. Fig. 4 displays considerable lack of agreement between the two instruments, with discrepancies of up to 4 for L^* and 25 for b^*. These differences are not obvious from Fig. 3. For the data, there is no obvious relation between the difference and the mean. Under these conditions, the lack of agreement can be reviewed by calculating the bias, estimated by the mean difference d (reference parameter minus target parameter) and the standard deviation of the differences s. If there is a consistent bias, the values can be adjusted by subtracting d from the data obtained by the target instrument. For the L^* data, d is 1.1 and s is 0.6. For the b* data, d is -3.1 and s is 5.0. The differences are expected to lie between the limits of agreement $d-2s$ and $d+2s$ (Fig. 4).These limits of agreement are -0.1 to 2.3 for the L^* data and -13.1 to 6.9 for the b^* data. For the two parameters L^* and b^*, many differences are outside the limits of agreement, so the results obtained by the two instruments are incompatible, hence the need to make prediction models.

Before any prediction procedure, the first step is to examine the data to calculate the mean absolute differences between the $L^*a^*b^*$ parameters of the reference instrument and those measured with the target instruments. By comparing the colorimeter with the Konica spectrophotometer, mean absolute differences are equal to 1.5 for L^*, 2.1 for a^* and 4.0 for b^*. As regards the HunterLab spectrophotometer, the mean absolute differences are equal to 4.6 for L^*, 2.2 for a^* and 4.0 for b^*.

To use the spectrophotometer target, the products assessed as conform with the colorimeter must also be assessed as conform i.e., that the parameter values measured by this spectrophotometer should be also within the tolerance range. Table 1 presents the $L^*a^*b^*$ parameters obtained with the colorimeter and with the spectrophotometers for two conformed samples. For some products, as differences from values obtained by colorimeter and by spectrophotometer being low, the new parameters values are still included in the range of tolerance; it is the case for sample 1. Nevertheless, for other products, as sample 2, assessed as conform with the colorimeter, because of the differences induced by the instrument change, the new values are outside the tolerance range, hence the need to make prediction models.

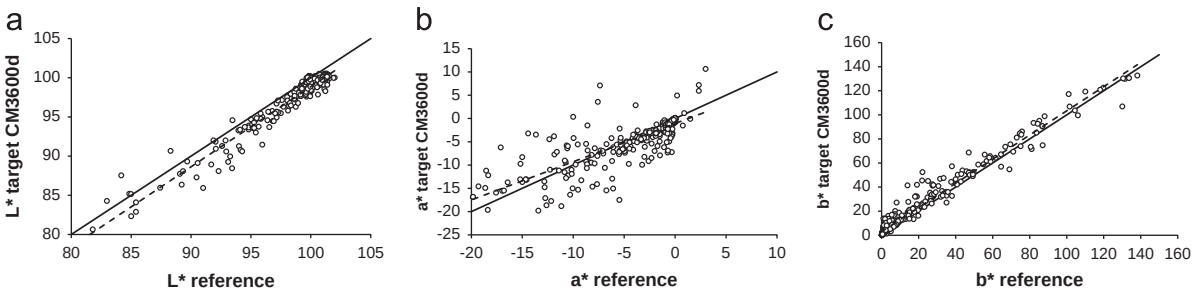

Fig. 3. Scatter diagram of (a) L^*, (b) a^* and (c) b^* for the CM3600d target instrument (—— line of equality, —— regression line).

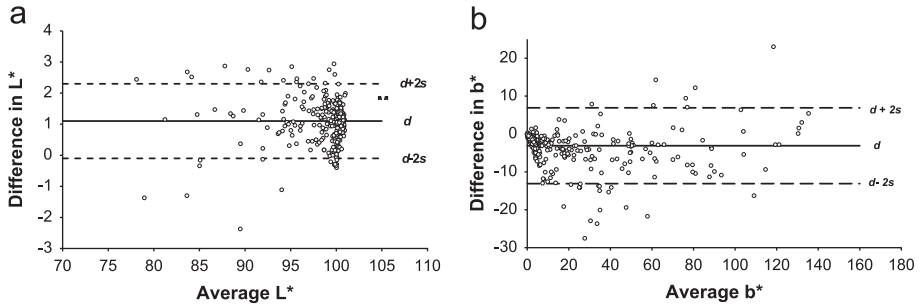

Fig. 4. Differences diagram of (a) L^* and (b) b^* values for the CM3600d target instrument.

Table 1
Preliminary comparison of the $L^*a^*b^*$ parameters between colorimeter and spectrophotometers for two conform samples.

Parameter (tolerance range)	Sample no. 1			Sample no. 2		
	L^* (87/97)	a^* (−9/1)	b^* (25/45)	L^* (77/87)	a^* (−13/−3)	b^* (45/65)
Colorimeter	93.46	−4.37	32.89	79.32	−3.87	65.00
Spectrophotometer Konica	94.57	−6.02	32.98	76.88	2.85	71.57
Spectrophotometer HunterLab	91.42	−5.94	32.28	74.06	2.48	69.25

4.1. Predictive model by simple linear regression

Linear regression models have been calculated to describe the relationship between L^* parameters of the CT310 and L^* parameters of the CM3600d, and between L^* parameters of the CT310 and L^* parameters of the UltraScan. The same procedure was made for the chromaticity coefficients a^* and b^*, as seen in Fig. 5.

In the case of the parameter L^*, Fig. 5(a, b) shows a strong correlation and a low relative error of prediction ($REP_{L^*}=1\%$) by linear regression. So, this model could be used to operate the prediction of L^* from data obtained by the target instruments. However, Fig. 5(b–e) shows that for the chromaticity coefficients a^* and b^*, REP are too high ($REP_{a^*}=90\%$, $REP_{b^*}=28\%$).

Fig. 2 shows a spectral overlap of the two areas of the color matching functions $x(\lambda)$ and $z(\lambda)$ between 380 and 510 nm. Despite this, these values are used to calculate the chromaticity coefficients a^* and b^* according to the transfer functions listed above (Eqs. (1–3)). This spectral overlap could explain these significant REP. These models are not reliable. Therefore, the prediction model creation requires a more elaborated processing than a simple linear regression.

The next logical step is to overcome this intermediate step of calculating the L^* a^* b^* parameters from the XYZ tristimulus values and operate the entire reflectance spectrum. To do so, the partial least squares (PLS) regression, is used. So, it we will be able to compare the L^* a^* b^* parameters obtained with the colorimeter and the reflectance spectra obtained with the target spectrophotometers.

4.2. Predictive model by partial least squares regression

In order to predict the samples $L^*a^*b^*$ parameters of samples, prediction models, based on reflectance spectra, calculated by PLS regression are performed on each parameter and for each target spectrometer. Results are given in Fig. 6. A mathematical model correlates the input variables, i.e., the reflectance values in the spectral range, and the responses to predict, i.e., the $L^*a^*b^*$ parameters.

Tables 2 and 3 give the ranges, the number of elements, the correlation coefficients and the errors of the models. By comparing the results of the models obtained for the two spectrophotometers, the prediction models are quite similar but the spectrophotometer Konica CM3600d gives a slightly better correlation. This can probably be attributable to the similarity in the sensor system arrangement employed in the Konica Minolta colorimeter and Konica Minolta spectrophotometer. To assess the reality of these differences, a Fisher–Snedecor test is performed on the two SEP respectively for the variables L^*, a^* and b^*. This test allows to affirm that the SEP are not statistically different at a significance level of 5%.

The results demonstrate that the PLS models obtained with the two spectrophotometers are quite similar and show significant correlations and good predictive abilities ($R^2 \geq 0.99$ and $0.9 < REP < 16$). Models are both satisfactory for the prediction, from the target instruments, of the three $L^*a^*b^*$ parameters of the reference instrument. REPs have been divided by 6 for the prediction of a^* and by 2 for the prediction of b^* compared to the prediction by linear regression.

To verify the dependency between L^*, a^* and b^* parameters, a regression test was performed by PLS2. PLS2 regression is a version of the PLS method in which it is possible to model several variables simultaneously, the three color space parameters here. This allows to assess whether correlations or collinearity between variables and thus determine their possible dependence. The results of testing by PLS2 show that this does not improve the prediction compared to the results obtained by PLS1; prediction errors are slightly above. This information does not yet allow to conclude on the independence of the parameters of the color space. When areas of reflectance spectra which contain the most information for the parameter to calculate (as shown on Fig. 2 and in the transfer Eqs. (1–3)) are selected and used to achieve the prediction models by PLS1 regression, prediction models are not improved. So, it is fair to say that the parameters of the $L^*a^*b^*$ color space are independent variables.

In some cases, the selection of informative spectral regions aims to construct better PLS models than those based on the overall spectral range. However, in this study, it did not improve predictive ability of PLS.

In addition to the REP calculation, conformity calculations were carried out on the 380 samples classified as conform in accordance with the reference instrument, that is to say the determination of the number of samples found not conform by the target instruments, and would therefore be rejected in terms of quality control. Table 4 summarizes the number of samples

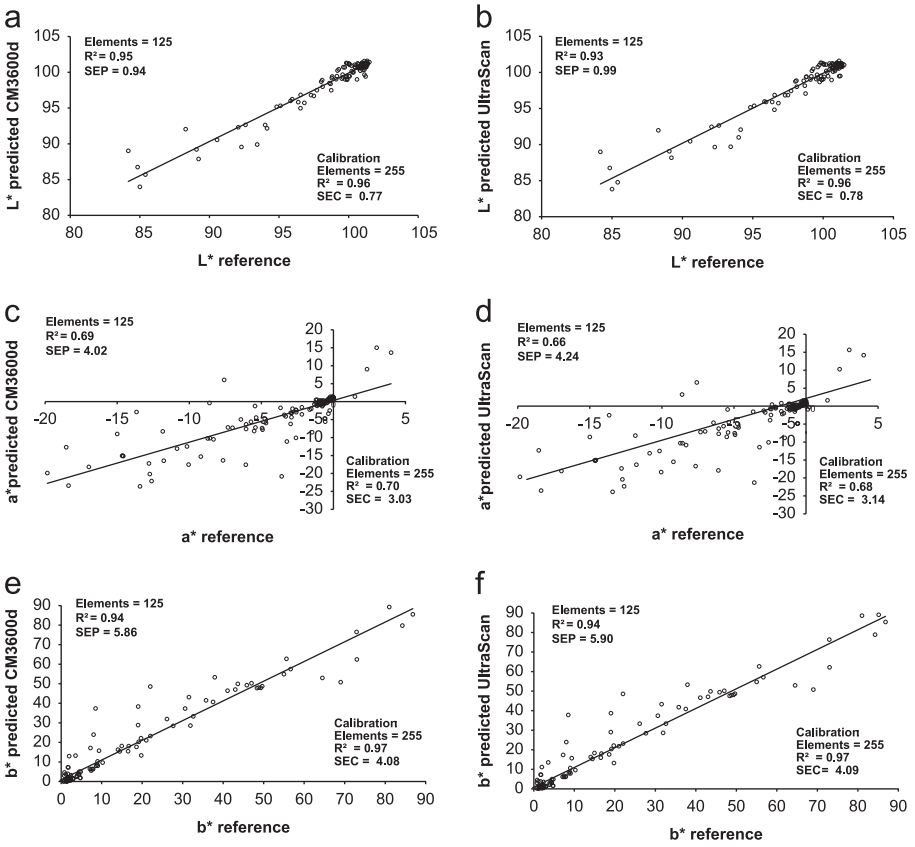

Fig. 5. Linear regression models for L^* (a) CM3600d, (b) UltraScan, for a* (c) CM3600d, (d) UltraScan and for b^* (e) CM3600d, (f) UltraScan.

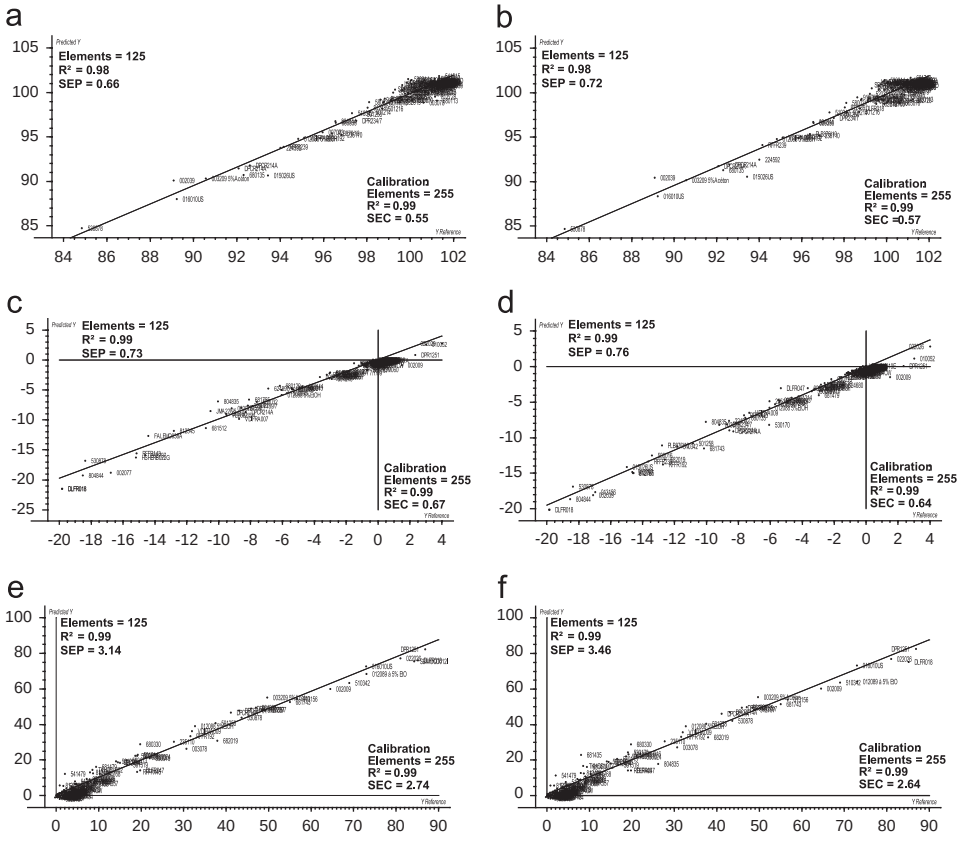

Fig. 6. PLS regression models for L^* (a) CM3600d, (b) UltraScan, for a^* (c) CM3600d, (d) UltraScan and for b^* (e) CM3600d, (f) UltraScan.

Table 2
Determination of $L^*a^*b^*$ parameters by PLS treatment of reflectance spectra from the Konica CM3600d spectrophotometer.

	L^*		a^*		b^*	
	Calibration	**Prediction**	**Calibration**	**Prediction**	**Calibration**	**Prediction**
Range (%)	60–102.0		−20–2		0.01–101	
Elements	268	132	255	125	255	125
Correlation	0.993	0.983	0.989	0.989	0.993	0.989
SEC SEP	0.75	0.86	0.67	0.73	2.74	3.14
REP(%) (LV)	0.9 (6)		15.5 (7)		14.9 (7)	

SEC: standard error of calibration, SEP: standard error of prediction, REP: relative error of prediction, LV: number of latent variables.

Table 3
Determination of $L^*a^*b^*$ parameters by PLS treatment of reflectance spectra from the HunterLab UltraScan spectrophotometer.

	L^*		a^*		b^*	
	Calibration	**Prediction**	**Calibration**	**Prediction**	**Calibration**	**Prediction**
Range (%)	60–102.0		−20–2		0.01–101	
Elements	268	132	255	125	255	125
Correlation	0.993	0.981	0.990	0.989	0.993	0.987
SEC SEP	0.75	0.91	0.67	0.76	2.64	3.46
REP(%) (LV)	0.9(6)		16.2(7)		16.4(7)	

SEC: standard error of calibration, SEP: standard error of prediction, REP: relative error of prediction, LV: number of latent variables.

Table 4
Number of samples wrongly classified as non-conform by the target instruments

Parameter (tolerance range)	**Konica Minolta CM-3600d**				**HunterLab Ultrascan**			
	L^* **(87/97)**	a^* **(−9/1)**	b^* **(25/45)**	**Rejected samples**	L^* **(77/87)**	a^* **(−13/−3)**	b^* **(45/65)**	**Rejected samples**
Non conform before treatment	26	39	52	88	338	47	49	347
Non conform after linear regression	0	18	28	30	1	20	27	33
Non conform after PLS regression	0	6	7	8	1	6	7	10

Table 5
Number of samples wrongly classified as non-conform for at least one parameter non conform by the target instruments.

Parameter (tolerance range)	**Konica Minolta CM-3600d** $L^*a^*b^*$	**HunterLab Ultrascan** $L^*a^*b^*$
Non conform before treatment	88	347
Non conform after linear regression	30	33
Non conform after PLS regression	8	10

wrongly classified as non-conform by the target instruments before and after treatment of the parameter values $L^*a^*b^*$ by linear regression and by PLS. A sample having a value out of range for at least one of the three parameters was rejected. With the Konica Minolta CM3600d instrument, 7% of the samples were rejected according to their out of range L^* value, 10% for a^* and 14% for b^*. The number of rejected samples reaches 23%. Some samples were defective according to several parameters, that is why the final number of rejected samples was less than the sum of the number of rejected samples according to one of the three parameters. An average of 38% of the samples was rejected with the Hunterlab UltraScan instrument due to a very poor concordance of this instrument with the reference instrument for the L^* values. The linear regression treatments greatly reduce the number of samples misclassified. With the Konica Minolta CM3600d instrument, neither sample was declassified and with the Hunterlab UltraScan instrument only one sample was declassified because of its wrong L^* value. With both instruments, there were only 6% and 7%, respectively of the a^* and b^* values that were found out of ranges. Finally, 8% of the samples were rejected with the Konica Minolta CM3600d instrument and 9% with the Hunterlab UltraScan instrument. PLS regression did not improve the L^* results but the number of rejected samples were reduce to 2% with the values predicted by the PLS regression Table. 5.

PLS regression is a more effective technique that can achieve better quality models than those obtained by linear regression. Indeed, the REP and the correlation coefficients indicate the predictive quality of the correlation models, which are not bad for a routine application. Finally, the best prediction models obtained are those made independently for the three parameters on the whole reflectance spectra by PLS1 regression.

5. Conclusion

The aim of the study was to be able to predict from the measured values of the target instruments, the values that would have resulted on the reference instrument with an error as small as possible, the final outcome is to enable the quality control laboratory to maintain its current control maps. To be done, it was necessary to provide the best prediction model between the reference instrument, a tristimulus colorimeter and the target ones, two bench-top sphere spectrophotometers.

On the basis of the results achieved in this work, predictive models of the CIE$L^*a^*b^*$ color space are feasible for the two spectrophotometry devices. The various chemometric tools tested show that the PLS1 regression applied on the entire reflectance spectra of each parameter of the color space is the one that achieves the best prediction models. These models can respond positively to the issue of replacement of laboratory equipment.

References

[1] D.B. MacDougall, Colour in Food: Improving Quality, Woodhead Publishing, 2002.
[2] H.A. Roth, L. Radle, S.R. Gifford, F.M. Clydesdale, J. Food Sci. 53 (1988) 1116–1162.
[3] C. Calvo, A. Salvador, S.M. Fiszman, Eur. Food Res. Technol. 213 (2001) 99–103.
[4] A.J. Meléndez-Martínez, I.M. Vicario, F.J. Heredia, Food Qual. Preference 16 (2005) 471–478.
[5] V.L.P. Ferreira, S.V. Fernandes, K. Yotsuyanagi, Rev. Esp. Cienc. Technol. Aliment. 34 (1994) 311–322.
[6] D. Ansorena, M.P. De Peña, I. Astiasarán, J. Bello, J. Meat Sci. 46 (1997) 313–318.
[7] A.J. Meléndez-Martínez, I.M. Vicario, F.J. Heredia, J. Agric. Food Chem. 51 (2003) 7266–7270.
[8] L. Dufossé, P. Galaup, E. Carlet, C. Flamin, A. Valla, Food Res. Int. 38 (2005) 919–924.
[9] M.J. Moyano, A.J. Meléndez-Martínez, J. Alba, F.J. Heredia, Food Res. Int. 41 (2008) 513–521.
[10] V.G. Mata, P.B. Gomes, A.E. Rodrigues, Ind. Eng. Chem. Res. 51 (2005) 2834–2852.
[11] J.C. Zwinkels, Displays 16 (1996) 163–171.
[12] B.S. Buslig, Proc. Fla. State. Hort. Soc. 104 (1991) 131–134.
[13] A. Fullerton, J. Keiding, Skin Res. Technol. 3 (1997) 237–241.
[14] A.J. MeléndezMartínez, I.M. Vicario, F.J. Heredia, J. Sci. Food Agric. 85 (2005) 894–901.
[15] G. Wyszecki, W.S. Stiles, Color Science: Concepts and Methods, Quantitative Data and Formulae, second ed., Wiley-Interscience, 2000.
[16] CIE, CIE 1976 L*a*b* Color Space, ISO 11664-4:2008(E)/CIE S 014-4/E (2007).
[17] CIE, CIE Tristimulus Values, CIE S 014-3/E (2011).
[18] K.M.M. Krishna Prasad, S. Raheem, P. Vijayalekshmi, C.Kamala Sastri, Talanta 43 (1996) 1187–1206.
[19] D. Isaacs Method and Apparatus for Color Spectrophotometry, Patent number 3874799 (1975).
[20] CIE, CIE Standard Illuminants for Colorimetry, ISO 11664-2:2007(E)/CIE S 014-2/E (2006).
[21] CIE, CIE Standard Colorimetric Observers, ISO 11664-1:2007(E)/CIE S 014-1/E (2007).
[22] S. Wold, H. Martens, H. Wold, The multivariate calibration problem in chemistry solved by the PLS method, Matrix Pencils, Springer Berlin Heidelberg, pp. 286–293.
[23] J.M. Bland, D.G. Altman, Lancet (1986) 307–310.